Positional Isotope Exchange Analysis of the Pantothenate Synthetase Reaction†

LaKenya Williams,‡ Renjian Zheng,§ John S. Blanchard,*,§ and Frank M. Raushel*,‡

Department of Chemistry, P.O. Box 30012, Texas A&M University, College Station, Texas 77842-3012, and Albert Einstein College of Medicine, 1300 Morris Park Avenue, Bronx, New York 10461

Received January 16, 2003; Revised Manuscript Received March 7, 2003

ABSTRACT: Pantothenate synthetase from *Mycobacterium tuberculosis* catalyzes the formation of pantothenate from ATP, D-pantoate, and β-alanine. The formation of a kinetically competent pantoyl-adenylate intermediate was established by the observation of a positional isotope exchange (PIX) reaction within ^{18}O-labeled ATP in the presence of D-pantoate. When [$\beta\gamma$-$^{18}O_6$]-ATP was incubated with pantothenate synthetase in the presence of D-pantoate, an ^{18}O label gradually appeared in the $\alpha\beta$-bridge position from both the β- and the γ-nonbridge positions. The rates of these two PIX reactions were followed by ^{31}P NMR spectroscopy and found to be identical. These results are consistent with the formation of enzyme-bound pantoyl-adenylate and pyrophosphate upon the mixing of ATP, D-pantoate, and enzyme. In addition, these results require the complete torsional scrambling of the two phosphoryl groups of the labeled pyrophosphate product. The rate of the PIX reaction increased as the D-pantoate concentration was elevated and then decreased to zero at saturating levels of D-pantoate. These inhibition results support the ordered binding of ATP and D-pantoate to the enzyme active site. The PIX reaction was abolished with the addition of pyrophosphatase; thus, PP_i must be free to dissociate from the active site upon formation of the pantoyl-adenylate intermediate. The PIX reaction rate diminished when the concentrations of ATP and D-pantoate were held constant and the concentration of the third substrate, β-alanine, was increased. This observation is consistent with a kinetic mechanism that requires the binding of β-alanine after the release of pyrophosphate from the active site of pantothenate synthetase. Positional isotope exchange reactions have therefore demonstrated that pantothenate synthetase catalyzes the formation of a pantoyl-adenylate intermediate upon the ordered addition of ATP and pantoate.

Pantothenate synthetase (EC 6.3.2.1) is an ATP-dependent enzyme that catalyzes the formation of the amide bond of pantothenate from D-pantoate and β-alanine in the final step of the pantothenate biosynthetic pathway (Scheme 1). Pantothenate, a member of the B group of vitamins, is a key precursor in the biosynthesis of coenzyme A and acyl carrier protein, two essential cofactors involved in numerous metabolic reactions (*1*, *2*). These reactions include fatty acid synthesis and oxidization, transcription, cell signaling, and the biosynthesis of polyketides and nonribosomal peptides (*3*−*7*). Pantothenate is synthesized de novo in bacteria, yeast, and plants, but mammals must obtain it from their diet (*1*). Pantothenate is synthesized via three enzymatic steps from α-ketoisovalerate, which is also an intermediate in the biosynthesis of the branched chain amino acids valine and leucine (*1*). The biosynthesis of pantothenate is essential for the growth of *Mycobacterium tuberculosis*, suggesting that the enzymes involved in the pantothenate biosynthetic pathway are appropriate targets for the development of antimycobacterial agents.

Scheme 1

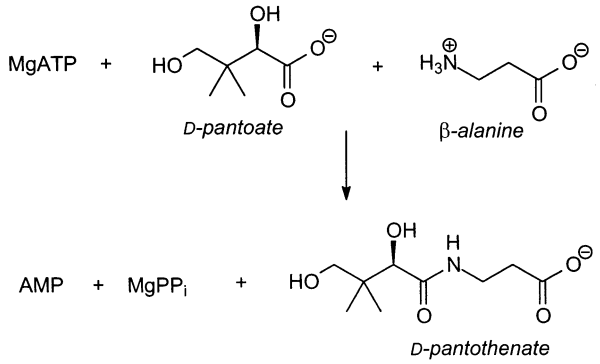

Pantothenate synthetase has been purified and partially characterized from *Escherichia coli*, *Lotus japonicus*, and *Oryza sativum* (*8*, *9*). Mg^{2+} is required for pantothenate synthetase activity, and the three-dimensional structure of unliganded *E. coli* pantothenate synthetase reveals that it is a member of the cytidylyltransferase family of enzymes (*9*, *10*). We have previously cloned, expressed, purified, and kinetically characterized pantothenate synthetase from *M. tuberculosis* (*11*). The enzyme is a homodimer with a subunit molecular weight of 33 kDa. The steady-state kinetic mechanism of the *M. tuberculosis* pantothenate synthetase is a Bi Uni Uni Bi Ping Pong mechanism, with ATP binding followed by D-pantoate binding, release of PP_i, binding of β-alanine, and finally the release of pantothenate and AMP. On the basis of this kinetic mechanism, the overall reaction

† This work was supported in part by grants from the National Institutes of Health (GM 33894 to F.M.R. and AI 33696 to J.S.B.) and the Robert A. Welch Foundation (A-840 to F.M.R.).

* Correspondence may be sent to the following authors. (F.M.R.) Telephone: (979) 845-3373. Fax: (979) 845-9452. E-mail: raushel@tamu.edu. (J.S.B.) Telephone: (718) 430-3096. Fax: (718) 430-8565. E-mail: blanchar@aecom.yu.edu.

‡ Texas A&M University.

§ Albert Einstein College of Medicine.

10.1021/bi0340853 CCC: $25.00
Published on Web 04/05/2003

Scheme 2

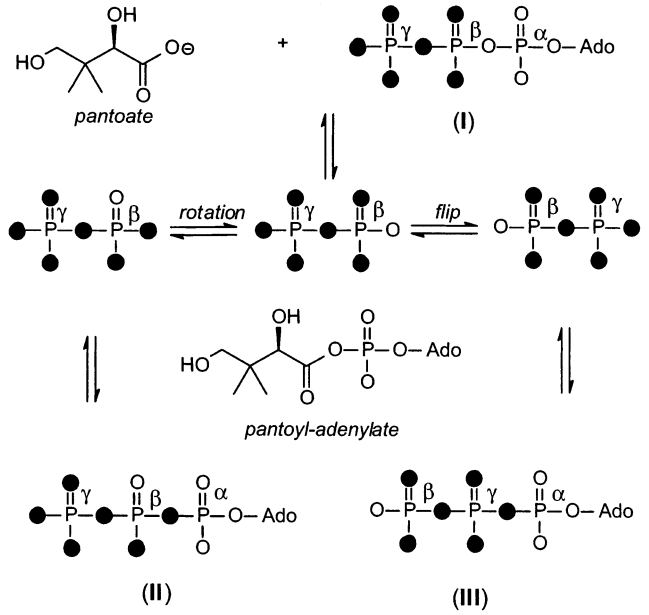

consists of two sequential steps, pantoyl-adenylate formation, and the subsequent nucleophilic attack on the mixed anhydride by β-alanine to form pantothenate (*8*, *11*). The formation of pantoyl-adenylate, proposed as a required intermediate in the kinetic mechanism, was supported by ^{31}P NMR spectroscopy of the product, [$^{18}O_1$]-AMP, produced by ^{18}O transfer to AMP from [carboxyl-$^{18}O_2$]-pantoate. The rates of the two single reactions (pantoyl-adenylate formation and breakdown) determined under presteady-state conditions are consistent with the rate of the overall reaction, indicating that pantoyl-adenylate is a kinetically competent intermediate (*11*).

The positional isotope exchange (PIX)[1] technique is a method that can be used to determine the kinetic competence of reaction intermediates and establish kinetic mechanisms in enzyme-catalyzed reactions (*12*−*14*). For example, the ordered binding of ATP and XMP during the reaction catalyzed by GMP synthetase was established by PIX experiments (*15*). The PIX reaction within [$\beta\gamma$-$^{18}O_6$]-ATP was observed with GMP synthetase only in the presence of XMP, and the exchange reaction did not require NH_3. Increasing concentrations of XMP suppressed the PIX reaction within the labeled ATP (*15*). PIX experiments have also been used to assess the obligatory formation of D-alanyl phosphate as an intermediate in D-Ala-D-X ligase reactions (*16*, *17*).

An outline of the two PIX reactions that could be catalyzed by pantothenate synthetase is presented in Scheme 2. When [$\beta\gamma$-$^{18}O_6$]-ATP (**I**) is incubated with D-pantoate in the presence of enzyme, PP_i and pantoyl-adenylate are anticipated to form within the active site. The oxygen-18 labels within the newly formed PP_i can positionally scramble via two possible routes from this intermediate complex. If there is unrestricted rotation about the bond connecting the bridging oxygen with the original β-phosphoryl group of the newly formed pyrophosphate, then an ^{18}O will eventually be found in the $\alpha\beta$-bridge position upon reformation and dissociation of ATP (**II**). Alternatively, if the PP_i that is formed within the active site can flip so as to interchange the positional identities of the original β- and γ-phosphoryl groups of ATP, then an ^{16}O will be found in the γ-phosphoryl group of ATP (**III**) upon reformation and dissociation of this labeled substrate. Therefore, if the rotation of the initially formed pyrophosphate product is unrestricted (either through dissociation/reassociation or tumbling within the active site), then an equilibrium mixture of ATP molecules will form with ^{18}O-labeling patterns represented by structures **I**, **II**, and **III**. However, if the PP_i is so tightly bound that only torsional equilibration of the β-phosphoryl group is kinetically significant, then the formation of **III** is not possible. In this case, isotopic equilibration would be restricted to the equilibrium formation of **I** and **II**. In this paper, we report the results of positional isotope exchange experiments using *M. tuberculosis* pantothenate synthetase to establish the participation of pantoyl-adenylate as a kinetically competent intermediate and to demonstrate that the PP_i is free to dissociate and then reassociate with the pantoyl-adenylate enzyme complex.

MATERIALS AND METHODS

Materials. Myokinase, carbamate kinase, pyrophosphatase, and β-alanine were purchased from Sigma Chemical Co. Oxygen-18 labeled water (90%) was obtained from Cambridge Isotope Laboratories. Oxygen-18 labeled potassium phosphate was prepared using the method outlined by Risley and Van Etten (*18*). The synthesis of [$\beta\gamma$-$^{18}O_6$]-ATP (**I**) was accomplished by following the procedure of Cohn and Hu with slight modifications (*19*). Pantothenate synthetase from *M. tuberculosis* was expressed in *E. coli* and purified as previously described (*11*). Phosphorus pentachloride and all other chemicals were purchased from Aldrich Chemical Co.

^{31}P Nuclear Magnetic Resonance Measurements. ^{31}P NMR spectra were acquired using a Varian Inova-400 multinuclear NMR spectrometer operating at a frequency of 162 MHz. Acquisition parameters were 5000-Hz sweep width, 6.0 s acquisition time, 2.0 s delay between pulses, 12.5 μs pulse width (pulse width 90° = 25 μs), and Waltz decoupling (35 db).

Positional Isotope Exchange Reaction. The positional isotope exchange reaction as a function of time was measured by following the incorporation of the β and/or γ-nonbridge oxygens from [$\beta\gamma$-$^{18}O_6$]-ATP (**I**) into the $\alpha\beta$-bridge position (Scheme 2). The reaction mixtures contained 10 mM [$\beta\gamma$-$^{18}O_6$]-ATP (**I**), 10 mM $MgCl_2$, 15 mM KCl, 0.1 mM D-pantoate, 50 mM HEPES, pH 7.8, and pantothenate synthetase at a final concentration of 13 μM. The volume of the assay mixture was 4.0 mL, and the sample was incubated at 30 °C for up to 8 h. Aliquots of 500 μL were removed every hour, and the reaction was quenched by adding two drops of CCl_4 with vigorous vortexing. The precipitated protein was removed by passage through a 0.45 μm Corning syringe filter and then concentrated to near dryness with the aid of a rotary evaporator. The material was then dissolved in a 750 μL solution containing 200 mM EDTA, pH 9.0 and 15% D_2O.

The [$\beta\gamma$-$^{18}O_6$]-ATP (**I**) was also incubated with various amounts of D-pantoate, β-alanine, and inorganic pyrophos-

[1] Abbreviations: HEPES, 4-(2-hydroxyethyl)-1-piperazine ethanesulfonic acid; PIX, positional isotope exchange.

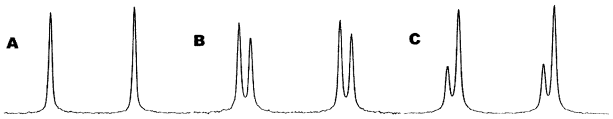

FIGURE 1: ^{31}P NMR spectra of the α-P of ATP. (A) $^{16}O_4$ species of [$\beta\gamma$-$^{18}O_6$]-ATP (**I**) at time zero; (B) after incubation with D-pantoate and pantothenate synthetase for 4 h; and (C) after incubation for 8 h. The new upfield signal within the doublet for the α-P is the resonance for the migration of an ^{18}O-label into the αβ-nonbridge position of ATP (as in structures **II** and **III**).

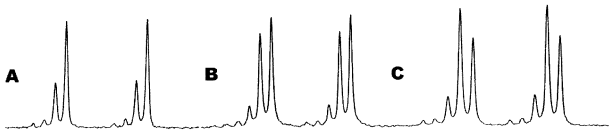

FIGURE 2: ^{31}P NMR spectra of γ-P of ATP. (A) The three resonances for the doublet of γ-P of the synthesized [$\beta\gamma$-$^{18}O_6$]-ATP (**I**) represent the species with 4, 3, and 2 atoms of ^{18}O at time zero; (B) after incubating with D-pantoate and pantothenate synthetase for 4 h; and (C) after incubating for 8 h.

phatase. Reactions with variable concentrations of D-pantoate contained 10 mM [$\beta\gamma$-$^{18}O_6$]-ATP (**I**), 10 mM $MgCl_2$, 15 mM KCl, 50 mM HEPES, pH 7.8, and D-pantoate ranging from 0.01 to 15 mM. The volume of the assays was 0.5 mL with an enzyme concentration of 13 μM. The reactions were incubated at 30 °C for 3 h and then quenched and treated as described above. Assays with the addition of inorganic pyrophosphatase contained 10 mM [$\beta\gamma$-$^{18}O_6$]-ATP (**I**), 10 mM $MgCl_2$, 15 mM KCl, 0.1 mM D-pantoate, 50 mM HEPES, pH 7.8, 13 μM pantothenate synthetase, and pyrophosphatase ranging from 0.001 to 10 units in a final volume of 0.5 mL. The reactions were quenched as previously outlined. The concentration of β-alanine was varied from 0.01 to 5.0 mM in reaction volumes of 0.5 mL containing 10 mM [$\beta\gamma$-$^{18}O_6$]-ATP (**I**), 10 mM $MgCl_2$, 15 mM KCl, 0.25 mM D-pantoate, 50 mM HEPES, pH 7.8, and 13 μM pantothenate synthetase.

RESULTS AND DISCUSSION

Enzymatic Synthesis of [$\beta\gamma$-$^{18}O_6$]-ATP. The oxygen-18 labeled ATP (**I**) was synthesized from isotopically labeled carbamoyl phosphate, AMP, a trace of ATP, adenylate kinase, and carbamate kinase (*16*). The ^{18}O content was quantified using ^{31}P NMR according to the procedure of Cohn and Hu (*19*). The ^{31}P resonances for the α- and γ-phosphoryl groups of the labeled ATP (**I**) are shown in Figures 1A and 2A, respectively. Only one resonance is observed for the α-P since none of the oxygen atoms attached directly to this phosphoryl group are labeled with ^{18}O. In contrast, there are three resonances (the most downfield peak is a contaminant) observed for the γ-P of ATP (**I**) because the ^{18}O-labeled water used in the synthesis of potassium phosphate was not 100%. The relative peak intensities for the three resonances are 0.69 ($^{18}O_4$), 0.27 ($^{18}O_3{}^{16}O$), and 0.04 ($^{18}O_2{}^{16}O_2$) (Figure 2A). The percentage of ^{18}O at the six atom positions within the ^{18}O-labeled ATP (**I**) is calculated from these spectral data to be 91%.

Pantoyl-Adenylate Formation. The formation of a pantoyl-adenylate intermediate during the pantothenate synthetase reaction was ascertained using the positional isotope exchange methodology as outlined in Scheme 2. Incubation of enzyme, D-pantoate, and ^{18}O-labeled ATP (**I**) enabled the positional scrambling of the ^{18}O-labels within the original ATP to be followed as a function of time in the absence of added β-alanine. Incorporation of ^{18}O into the αβ bridge position of ATP (as in structure **II**) can only be observed if the original β-phosphoryl group of the newly formed pyrophosphate product can freely rotate within the active site of the enzyme. Alternatively, if the symmetrical PP_i can also flip end-over-end within the active site of pantothenate synthetase, then the positional orientation of the original β- and γ-phosphoryl groups will be lost, and an ^{16}O will then also appear in the γ-phosphoryl group of ATP (as in structure **III**). With either scenario, a new upfield resonance signal will appear in the NMR signal for the α-P (representing the α-P that now contains a single ^{18}O atom) as the reaction progresses, while the original resonance signal (containing no ^{18}O) will decrease. This new resonance is shifted 0.017 ppm upfield from the resonance for the all ^{16}O-labeled material (*19*). If the PP_i product is able to fully reorient itself within the active site, then there will also be an increase in the relative resonance signal for the [γ-$^{18}O_3{}^{16}O_1$]-P species and a decrease for [γ-$^{18}O_4$]-P. Figure 1 illustrates the change in isotopic composition for the α-P of ATP upon the incubation of enzyme, ATP (**I**), and D-pantoate. There is a decrease in the percentage of the original ^{16}O species (shown in Figure 1A) to 54 and 33% after 4 and 8 h, respectively (Figure 1B,C).

The rate constants for the approach to positional isotopic equilibrium at the α-P were obtained by fitting the experimental time course data to eqs 1 and 2. In these two equations, X_o is the amount of the [α-$^{16}O_4$]-P species at time t, X_t is the total NMR signal for all of the α-P species, z is the fraction of ^{18}O-labeling, n is the number of labeled compounds in pool 2, m is the number of labeled compounds in pool 1, and X_1 is the amount of the [α-$^{18}O_1{}^{16}O_3$]-P species at time t. For the mechanism that appears in Scheme 2 where only the rotation of the β-phosphoryl group is allowed, $n = 2$ and $m = 1$. However, if the pyrophosphate product is able to freely flip, then $n = 5$ and $m = 1$. Fitting the experimental data to eqs 1 and 2 yields a rate constant of 0.24 ± 0.03 hr^{-1} for the model ($n = 5$ and $m = 1$) where pyrophosphate is freely able to tumble within the active site (Figure 3).[2] The turnover number for the PIX reaction under these conditions was calculated to be 3.1 ± 0.4 min^{-1} using an enzyme concentration of 13 μM and an ATP concentration of 10 mM. This value may be compared to the determined k_{cat} of 3.4 ± 0.2 s^{-1} and the maximal rate of pantoyl-adenylate formation of 1.3 ± 0.3 s^{-1} (*11*).

The change in the isotopic composition of the γ-P was monitored by measuring the fractional decrease of the [γ-$^{18}O_4$]-P species and is presented in Figures 2 and 4. At time zero, the fraction of the [γ-$^{18}O_4$]-P species is 68% of the total NMR signal for the γ-P of ATP (Figure 2A). After 4 and 8 h, this fraction decreases to 48 and 38%, respectively (Figure 2B,C). The rate constant for the approach to positional isotopic equilibrium at the γ-P was obtained from a fit of the data to eq 3. In this equation, Y_4 is the amount of the [γ-$^{18}O_4$]-P species at time t, Y_t is the sum of all isotopic species for the γ-P, and all of the other values are the same as previously defined where $n = 1$ and $m = 1$. Fitting these

[2] A fit of these data to eqs 1 and 2 for the alternative model ($n = 2$ and $m = 1$) gave a rate constant of 0.4 ± 0.1 h^{-1}.

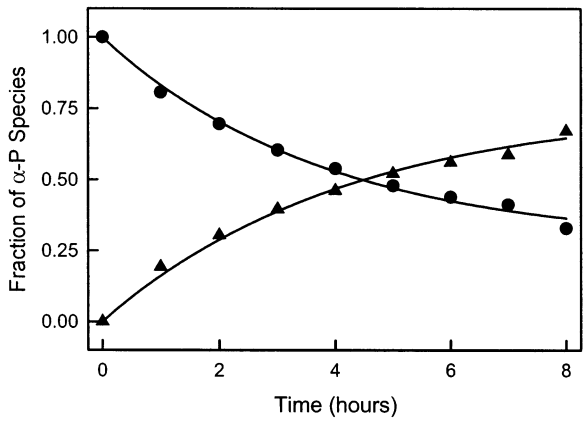

FIGURE 3: Time course for the PIX reaction at the α-phosphoryl of ATP (**I**). (●) Changes in the fraction of the [α-$^{16}O_4$]-P species as a function of time. (▲) Changes in the fraction of the [α-$^{18}O_1{}^{16}O_3$]-P species as a function of time. The solid lines are for a fit of the data to eqs 1 and 2. Additional details are provided in the text.

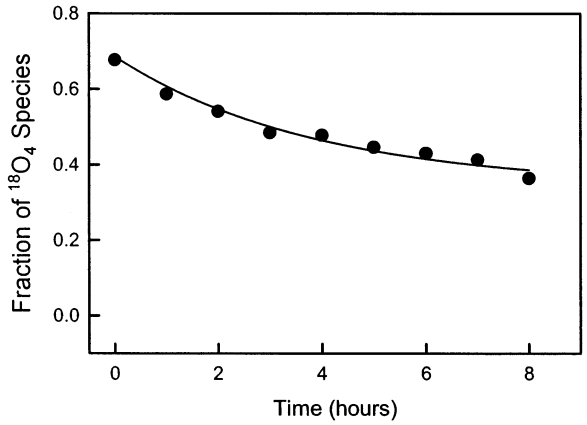

FIGURE 4: Time course for the PIX reaction at the γ-phosphoryl of ATP (**I**). The fraction of [γ-$^{18}O_4$]-P is plotted as a function of time. The data were fit to eq 3. Additional details are provided in the text.

data to eq 3 yields a rate constant of 0.24 ± 0.01 hr^{-1} (Figure 4), which gives a turnover number for the positional isotope exchange of 3.1 ± 0.1 min^{-1} using an enzyme concentration of 13 μM with an initial ATP concentration of 10 mM. Since the rate constants for the turnover of the positional isotope exchange reactions for the α-P and γ-P are identical, it is concluded that the rotation of pyrophosphate is unrestricted relative to the rotation of the β-phosphoryl group.

$$\frac{X_o}{X_t} = 1 + \frac{zne^{-kt}}{n+m} - \frac{zn}{n+m} \quad (1)$$

$$\frac{X_1}{X_t} = \frac{zn}{n+m} - \frac{zne^{-kt}}{n+m} \quad (2)$$

$$\frac{Y_4}{Y_t} = z^4\left(1 + \frac{ne^{-kt}}{n+m} - \frac{n}{n+m}\right) \quad (3)$$

Dissociation of Pyrophosphate. The PIX rates at the α- and γ-P positions of ATP are identical. This result is consistent with a complete reorientation of the pyrophosphate product within the active site of pantothenate synthetase upon formation of the pantoyl-adenylate intermediate. This result, however, does not distinguish between a model that allows for the pyrophosphate intermediate to partition between the active site and the bulk solution from a model that only allows for the rotational scrambling of the pyrophosphate completely within the confines of the active site. To determine whether the PP_i can dissociate from the active site of pantothenate synthetase, the PIX reaction was monitored in the presence of pyrophosphatase. If PP_i dissociates from the active site of the enzyme, the addition of pyrophosphatase will prevent the reassociation of PP_i through hydrolytic cleavage to phosphate. The destruction of PP_i will serve to suppress the PIX reaction. Alternatively, if PP_i flips within the active site without dissociation in the bulk solution, inclusion of inorganic pyrophosphatase in the assay mixture will have no effect on the rate of the observed PIX reaction. In these experiments, the PIX exchange rates (v) were calculated using eq 4 (*20*), where A is the initial concentration of labeled ATP, and F is the fraction of positional isotope scrambling equilibrium at time *t*. Shown in Figure 5 is the effect on the reaction rate as the concentration of pyrophosphatase is varied. The PIX rate is diminished to an undetectable level upon addition of as little as 0.1 units of pyrophosphatase to the reaction mixture. These results clearly demonstrate that the pyrophosphate product, formed in the presence of the pantoyl-adenylate intermediate, freely dissociates from the active site into the bulk solution.

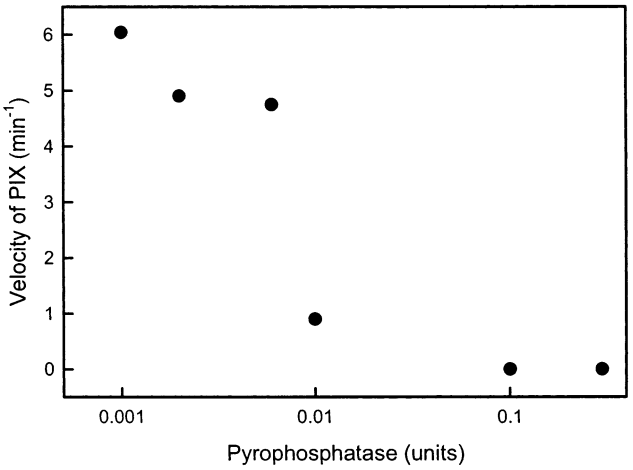

FIGURE 5: Effect of inorganic pyrophosphatase on the rate of the PIX reaction at the γ-P of ATP (**I**). Additional details are provided in the text.

$$v = -\left(\frac{A}{t}\right)\ln(1 - F) \quad (4)$$

The experiments reported in this paper demonstrate that essentially all of the PIX observed with pantothenate synthetase derives from the dissociation/reassociation of the ^{18}O-labeled pyrophosphate and resynthesis of ATP. The lack of a significant PIX reaction between the α- and the β-phosphoryl group from the torsional rotation of the β-phosphoryl group prior to pyrophosphate dissociation can arise from a variety of circumstances. For example, the pyrophosphate when bound to the active site may be torsionally rigid due to ionic interactions with the protein and/or divalent cations. The absence of any PIX reaction catalyzed by argininosuccinate synthetase was attributed to restricted bond rotation imposed by the protein (*21*). Alter-

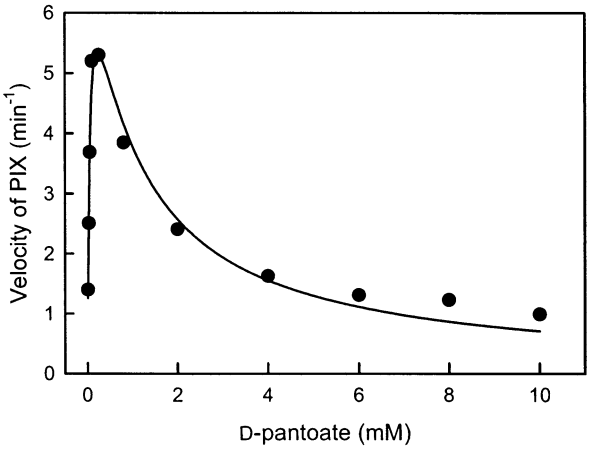

FIGURE 6: Effect of changing the concentration of D-pantoate on the rate of the PIX reaction. The rate of PIX reaction at the γ-P as a function of the concentration of D-pantoate was fit to eq 5. Additional details are provided in the text.

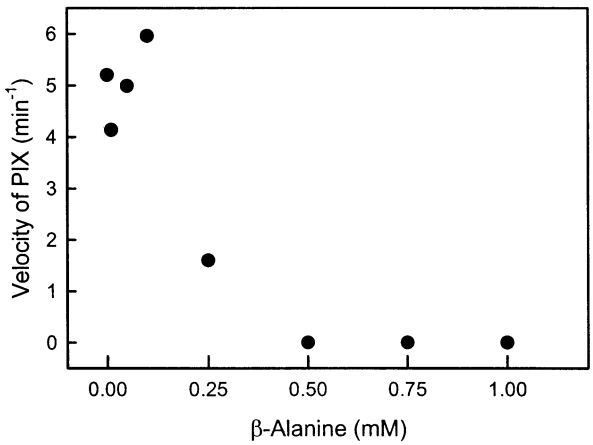

FIGURE 7: Effect of changing the β-alanine concentration on the rate of the PIX reaction.

natively, the ratio of the PIX reactions within pantothenate synthetase may be dictated by the rate of release of pyrophosphate into solution relative to the torsional rotation of the β-phosphoryl group and resynthesis of the ^{18}O-scrambled ATP. The kinetics of the PIX reaction catalyzed by methionyl-tRNA synthetase has been measured (*22*). With that enzyme, the overall PIX rate that occurred via the direct torsional scrambling of the β-phosphoryl group was about twice the contribution from the tumbling or flipping of the PP_i within the active site (*22*).

Inhibition of PIX by D*-Pantoate.* The rate of PIX in enzyme catalyzed reactions is often dependent on the concentration of the unlabeled substrates (*14*, *23*). The first sequential step in the postulated catalytic mechanism of pantothenate synthetase is the formation of the pantoyl-adenylate intermediate. If the binding of D-pantoate must follow the association of ATP to the free enzyme, then elevated concentrations of D-pantoate can either inhibit or abolish the observation of PIX (*14*, *23*). If the binding of ATP and D-pantoate is strictly ordered, the PIX reaction will be abolished since the ATP must be free to dissociate back into the bulk solution before any PIX can be observed. However, if the binding of ATP and D-pantoate is only partially ordered, then the PIX rate will be diminished but not abolished in the presence of very high concentrations of D-pantoate (*23*). The observed effect on the PIX reaction rate with changes in the initial D-pantoate concentration is presented in Figure 6. The variation of the PIX reaction velocity as a function of the pantoate concentration was fit to eq 5 (*24*) where B represents the concentration of D-pantoate, K_b is the enhancement constant, and K_i is the inhibition constant for the effect induced by D-pantoate. For the PIX reaction at the γ-phosphoryl group, $K_b = 0.05 \pm 0.01$ mM and $K_i = 1.0 \pm 0.2$ mM. These results are fully consistent with the ordered kinetic mechanism as determined from steady-state measurements (*11*).

$$v = \frac{VB}{K_b + B + \frac{B^2}{K_i}} \quad (5)$$

Inhibition of PIX by β*-Alanine.* The second sequential step of the proposed catalytic mechanism of pantothenate synthetase is the release of PP_i and binding of β-alanine. If the binding of β-alanine occurs after pantoyl-adenylate formation and PP_i release, then increasing the concentration of β-alanine should suppress the PIX activity. The overall effect of varying the concentration of β-alanine on the PIX reaction rate is presented in Figure 7. At elevated levels of β-alanine the PIX rate is diminished to zero. Again, these results are consistent with the proposed kinetic mechanism and steady-state measurements (*11*).

Summary. The PIX technique has proven to be a versatile tool during the elucidation of kinetic mechanisms and identification of reaction intermediates in enzyme catalyzed reactions. The postulated kinetic and chemical mechanisms of *M. tuberculosis* pantothenate synthetase (*11*) have been confirmed by the PIX experiments presented in this paper. This enzyme catalyzes a PIX reaction within [$\beta\gamma$-$^{18}O_6$]-ATP in the presence of D-pantoate. The total inhibition of the PIX reaction by increasing concentrations of D-pantoate and β-alanine confirms the ordered binding of these two substrates. The suppression of the PIX activity upon the addition of small amounts of pyrophosphatase establishes the free dissociation of PP_i from the enzyme/pantoyl-adenylate complex. However, attempts to directly observe a ^{31}P NMR signal for the pantoyl-adenylate intermediate were unsuccessful.

REFERENCES

1. Neidhardt, F. (1996) *Escherichia coli and Salmonella typhimurium*: *cellular and molecular biology*, 2nd ed., Vol. 1, pp 687−694, American Society for Microbiology, Washington, DC.
2. Abiko, Y. (1975) Metabolism of Coenzyme A, in *Metabolic Pathways* (Greenburg, D. M., Ed.) Academic Press, Inc., New York.
3. Mishra, P. K., and Drueckhammer, D. G. (2000) *Chem. Rev. 100*, 3283−3309.
4. DiRusso, C. C., Heimert, T. L., and Metzger, A. K. (1992) *J. Biol. Chem. 267*, 8685−8691.
5. Korchak, H. M., Kane, L. H., Rossi, M. W., and Corkey, B. E. (1994) *J. Biol. Chem. 269*, 30281−30287.
6. Dreier, J., Shah, A. N., and Khosla, C. (1999) *J. Biol. Chem. 274*, 25108−25112.
7. Lambalot, R. H., Gehring, A. M., Flugel, R. S., Zuber, P., LaCelle, M., Marahiel, M. A., Reid, R., Khosla, C., and Walsh, C. T. (1996) *Chem. Biol. 3*, 923−936.
8. Miyatake, K., Nakano, T., and Kitaoka, S. (1978) *J. Nutr. Sci. Vitaminol. 24*, 243−253.
9. Genschel, U., Powell, C. A., Abell, C., and Smith, A. G. (1999) *Biochem. J. 341*, 669−678.

10. von Delft, F., Lewendon, A., Dhanaraj, V., Blundell, T. L., Abell, C., and Smith, A. G. (2001) *Structure 9*, 439−450.
11. Zheng, R., and Blanchard, J. S. (2001) *Biochemistry 40*, 12904−12912.
12. Midelfort, C., and Rose, I. A. (1976) *J. Biol. Chem. 251*, 5881−5888.
13. Raushel, F. M., and Villafranca, J. J. (1988) *Crit. Rev. Biochem. 23*, 1−26.
14. Mullins, L. S., and Raushel, F. M. (1995) *Methods Enzymol. 249*, 398−425.
15. von der Saal, W., Chrysler, C. S., and Villafranca, J. J. (1985) *Biochemistry 24*, 2343−5350.
16. Healy, V. L., Mullins, L. S., Li, X., Hall, S. E., Raushel, F. M., and Walsh, C. T. (2000) *Chem. Biol. 7*, 505−514.
17. Mullins, L. S., Zawadzke, L. E., Walsh, C. T., and Raushel, F. M. (1990) *J. Biol. Chem. 265*, 8993−8998.
18. Risley, J. M., and Van Etten, R. L. (1978) *J. Labeled Compd. Radiopharm. 15*, 533−538.
19. Cohn, M., and Hu, A. (1980) *J. Am. Chem. Soc. 102*, 913−916.
20. Wimmer, M. J., Rose, I. A., Powers, S. G., and Meister, A. (1979) *J. Biol. Chem. 254*, 1854−1859.
21. Hilscher, L. W., Hanson, C., Russell, D. W., and Raushel, F. M. (1985) *Biochemistry 24*, 5888−5893.
22. Lowe, G., Sproat, B. S., and Tansley, G. (1983) *Eur. J. Biochem. 130*, *341−345*.
23. Hester, L. S., and Raushel, F. M. (1987) *Biochemistry 26*, 6465−6471.
24. Cleland, W. W. (1967) *Adv. Enzymol. Relat. Areas Mol. Biol. 29*, 1−32.

BI0340853